Multiple Forward Mode Canopy Reflectance Model Inversion for Above Ground Forest Biomass, Alberta Rocky Mountains

Scott A. Soenen [1], Derek R. Peddle [1], Ronald J. Hall [2,1] Craig A. Coburn [1]

[1] Department of Geography, University of Lethbridge, 4401 University Drive West
Lethbridge, AB, Canada T1K 3M4
Em: scott.soenen@uleth.ca

[2] Natural Resources Canada, Canadian Forest Service, 5320 – 122 Street
Edmonton, AB, Canada T6H 3S5

ABSTRACT

The amount and spatial distribution of aboveground forest biomass (AGB) are required inputs to forest carbon budgets and ecosystem productivity models. While emerging satellite remote sensing data and empirical methods can estimate forest canopy structure and AGB, they do so to varying degrees of success, and few of these methods can account for the effects of terrain on observed reflectance. The presence of terrain can affect the accuracy of estimates in sub-alpine and montane environments. This paper introduces a new method for obtaining AGB from forest structure estimates using a multiple-forward-mode (MFM) canopy reflectance model inversion that include constraints that account for the effects of terrain. This approach first estimates average tree crown dimensions and stem density for satellite image pixels through indirect inversion of a geometric-optical canopy reflectance model. These crown dimension and stem density estimates are then related to average tree biomass and AGB for the pixel. The estimates of AGB from the MFM approach were evaluated for 40 field validation sites at Kananaskis, Alberta, along the eastern slopes of the Canadian Rocky Mountains. On average, AGB estimates were within 50 tonnes/ha (RMSE) of the field plot values where biomass ranged from 70 to 250 tonnes/ha. This result was similar, or an improvement over other NDVI and Spectral Mixture Analysis empirical methods tested.

INTRODUCTION

Information about forest stand structure and aboveground biomass (AGB) is used for estimating forest ecosystem productivity, carbon (C) budgets, and to assess the role of forests in the global C cycle (Kurz and Apps, 1999; Cihlar et al., 2002; Palacios-Orueta et al., 2005). Currently, the most established and frequently used methods for estimating AGB use field plots or spatial inventory data with statistical or allometric models (Parresol, 1999; Brown, 2002). These conventional methods are difficult to extend over large areas because they are limited to where inventory data are available. Further, these methods may not be suited for future C reporting since the assessment is often done at only a single point in time (Brown, 2002; Hall et al., 2006). Alternatively, emerging satellite remote sensing methods are potentially well suited for providing efficient and timely estimates of forest structure and AGB due to the ability to provide both archived and new systematic, repetitive observation at local to global scales (Patenaude et al., 2005).

Although a number of remote sensing techniques for estimating stand structure and AGB have been reported, the variability in results suggests it remains a difficult, challenging task (Hyyppä et al. 2000; Foody et al. 2003; Rosenqvist et al., 2003; Lu 2006). Statistical techniques are among those most commonly used, whereby multispectral satellite data or derived information (e.g. vegetation indices, mixture fractions) are related empirically to stand structure and biomass (Wulder 1998; Gerylo et al., 2002; Hall et al., 2006). Some success has been reported in applications of these methods to areas of limited terrain relief (Hame et al., 1997; Peddle et al., 2001a; Gerylo et al., 2002; Franklin et al., 2003; Hall et al., 2006). The relationships between satellite data and stand characteristics, however, can be adversely influenced in areas of high topographic variation (Gemmell, 1995; 1998), or in areas where surface features

such as exposed rock and soil can lead to mixed pixels that can confound the relationship with biomass (Elvidge et al., 1985).

An alternative to statistical methods is the inversion of canopy reflectance models. Geometric-optical canopy reflectance models, in particular, provide a direct physical explanation of the relationship between forest stand structure, terrain structure, view angle, illumination angle, and the radiometric response of satellite data (Chen et al., 2000). Inversion of these models to provide information about forest stand structure has shown some promising results (Wu and Strahler, 1994; Woodcock et al., 1997), however, the inversion procedure can be computationally intensive and thus inappropriate for large study areas and time sensitive accounting. Further, some canopy reflectance models are not invertible, particularly those with increased model, required in complex terrain. Instead, to facilitate forest information extraction from non-invertible models, and to otherwise increase the efficiency of model inversion, it is necessary to use indirect inversion methods where canopy reflectance is pre-computed (Kimes et al., 2000). The look-up table method has been successfully tested in agricultural (Weiss et al., 2000), and forested settings (Peddle et al., 2003) for physical structure and dimensions, but it has not yet been used to estimate second-order physical parameters such as AGB.

This paper introduces a new method for estimating AGB from satellite imagery over mountainous terrain using canopy reflectance models that account for variation in reflectance due to either varying topography or an off-nadir observation-angle. This approach first estimates average tree crown dimensions and stem density for a satellite image pixel through indirect inversion of a geometric-optical canopy reflectance model, then it relates the crown dimensions and stem density to average tree biomass and AGB for the pixel. The objectives of this study were to:

(i) Describe this two-step canopy reflectance model based approach;
(ii) Evaluate the estimates against AGB field estimates collected in a mountainous study area; and
(iii) Compare the canopy reflectance model approach to other multispectral image-based approaches including spectral mixture analysis and use of vegetation indices (Peddle et al., 2001a).

The canopy reflectance model approach was hypothesized to generate more accurate estimates of AGB than those from multispectral image-based approaches through reference to independent field validation.

METHODS

Study area

The study area, centered at 51.02° N, 115.07° W, was located in Kananaskis Country Provincial Park, Alberta, Canada. Terrain elevations ranged from 1400m to 2100m above sea level with slopes ranging from 0° to 55° over a full range of terrain aspect. The study area included both Montane and Sub-Alpine vegetation zones (Archibald et al., 1996). The dominant overstory coniferous species were lodgepole pine (*Pinus contorta* var. *latifolia* Dougl ex. Loud.), white spruce (*Picea glauca* (Moench) Voss), Engelmann spruce (*Picea engelmannii* Parry ex Engelm.), Douglas-fir (*Pseudotsuga menziesii* (Mirb.) Franco), and subalpine fir (*Abies lasiocarpa* (Hook) Nutl.). The dominant deciduous tree species included trembling aspen (*Populus tremuloides* Michx.), and balsam poplar (*Populus balsamifera* L.), with lesser amounts of white birch (*Betula papyrifera* Marsh.).

Field data

Field data from 36 field plots were collected during two field seasons in 2003 and 2004. Of the 36 field plots, 21 were located within conifer dominant (>80% stem count) stands and 15 were located within deciduous dominant stands. Plot size was set at 0.04 ha to ensure at least one image pixel would coincide spatially with each plot. To ensure an adequate representation of the range of terrain and stand density conditions within the study area, field plot location was pre-selected based on DEM derivatives and information from the Alberta Vegetation Inventory (Alberta Environmental Protection, 1991). AGB validation data were calculated for each plot from field measurements of diameter at breast height (dbh) and tree heights. Other data, including crown dimensions and vegetation spectral response, were recorded to constrain canopy reflectance model parameterization and to validate initial inversion results.

Measurements of total tree height, height to center of the crown (HTC), dbh, horizontal, and vertical crown radius were taken for each tree within a field plot. In addition, species data and stem counts

for each plot were recorded. Tree heights and height to center of crown were measured using a digital clinometer at 20 m distance. Vertical crown radius was determined by subtracting the height to the base of the canopy (a parameter easily and accurately measured) from the total height, and dividing in half. To obtain HTC, the height to the base of the canopy was added to the vertical crown radius. The horizontal crown radius for each tree was measured using a GRS densiometer to determine the vertical projection of the edges of the crown to the ground (i.e. the drip-line). The distance from the drip-line back to the trunk was then measured. This process was repeated perpendicular to the first measurement to characterize variation in horizontal crown dimensions.

Spectral measurements were acquired for leaf (needle) samples from each of the overstory species and understory vegetation, and processed following protocols by Peddle et al. (2001b). An Analytical Spectral Devices (ASD) Field Spec Full-Range spectroradiometer (ASD, 1998) was used to record the spectral properties of sunlit and shadowed vegetation samples. The measurements occurred near the expected satellite overpass time on two cloudless dates in June and July, 2004. To ensure a high signal to noise ratio, the spectroradiometer was configured to acquire 10 measurements within one minute. These measurements were then averaged for each sample. Dark current calibrations and white reference measurements were completed prior to each target measurement to account for any internal signal noise and to capture illumination (irradiance) variations during measurement. To incorporate the field spectra in subsequent satellite image data processing, the spectral dimensionality was reduced by integrating the reflectance across a range of wavelengths corresponding to each SPOT band width, based on published spectral response functions for the satellite sensor (SPOT Image, 2004).

Estimating tree biomass from field data

Destructive sampling was not permitted within the Kananaskis study area to derive tree biomass (B). Instead, above ground total individual tree biomass was calculated for each tree within plot boundaries using dbh within the log-transformed power model and regression coefficients from Case and Hall (*in review)*:

$$ln(B) = b_0 + b_1 ln(\text{dbh}) \quad (1)$$

It was necessary to apply a correction factor to account for the skewness in the distribution in arithmetic units when converting from the logarithm of tree biomass to original biomass units (Baskerville, 1972). The B (tonnes·tree^{-1}) was then summed for each plot and divided by the plot area to give total biomass (tonnes) within the plot and total standing AGB (tonnes·ha^{-1}).

Image and terrain data

Système pour l'Observation de la Terre (SPOT) multispectral satellite imagery covering the study area was acquired under cloud free conditions 12 August 2003 by the High Geometric Resolution (HGR) SPOT 5 sensor at a -7.3° off-nadir view angle and 10m spatial resolution. The SPOT data were resampled to 25m to match the resolution of an associated digital elevation model (DEM) and orthorectified to within 5m positional error based on an independent ground control point based assessment. After orthorectification, the image data were converted from digital count to reflectance using published gain values, solar irradiance, and illumination geometry (SPOT Image, 2004). A correction based on pseudo-invariant features such as a parking lot calibration site (Milton et al., 1997) was also applied to account for the potential effects of atmospheric transmission and path radiance (Smith and Milton, 1999). All SPOT image bands were used within the canopy reflectance modeling procedure.

Multiple forward mode retrieval of canopy structural parameters

The SPOT image data were linked to forest canopy structural conditions using the multiple-forward-mode (MFM) canopy reflectance model inversion method (Peddle et al., 2003, 2007) and the Li-Strahler (1992) geometric- optical, mutual shadowing canopy reflectance model (GOMS). The MFM method is an indirect, look-up table based approach (Kimes et al., 2000) to canopy reflectance model inversion that consists of a set of algorithms for look-up table creation (Peddle et al., 2003), look-up table search and description of potential inversion solutions (Soenen et al., 2007b). MFM has been applied successfully in retrieval of structural parameters (Peddle et al., 2003; Soenen et al., 2007b), unsupervised classification (Peddle et al., 2004) and topographic correction (Soenen et al., 2005, 2007a). A detailed description of the MFM method has been provided by Peddle et al. (2003, 2007) and Soenen et al., (2007b), however, a brief description of the use of MFM in this study is provided next.

In the first MFM stage (Fig. 1), look-up tables were created for each of the four image bands from a set of model input canopy structure, viewing and illumination angles and terrain orientation parameters and the corresponding modeled reflectance output. A range and increment size was selected for each model input parameter from which the parameter sets were generated for the iterative model runs (Table 1). Two input parameter sets were used for each species: 1) a general range of structure covering the full range of potential canopy conditions in the area; and 2) a refined range of structure constrained by two standard deviations from the mean of the observed field structure conditions. The first parameter set simulated limited knowledge of field conditions, and the second parameter set was used to determine if improvements in prediction accuracy could be obtained with a refined parameter set. Each entry in the look-up table was created through a forward-mode execution of the GOMS model using the structural parameter sets as input. The resulting look-up tables contained all possible structural input parameter combinations and the modeled GOMS reflectance values for each satellite image band.

Table 1 – Model input

		Unconstrained			**Constrained**		
	Structural Parameter	*Min*	*Max*	*inc*	*Min*	*Max*	*inc*
Lodgepole Pine	Density - λ (trees/m^2)	0.05	0.5	0.05	0.06	0.26	0.02
	Horizontal Crown Radius - r (m)	0.5	6.5	1	0.5	2.5	0.5
	Vertical Crown Radius - b (m)	0.5	6.5	2	1	4	1
	Height to Crown Center - h (m)	4	14	2	10	14	1
	Height Distribution - dh (m)	5	25	5	6	16	2
	Slope - α (°)	0	60	10	0	40	5
	Aspect - φ (°)	0	315	45	0	315	45
	Size of parameter set		529200			445500	
Trembling Aspen	Density - λ (trees/m^2)	0.05	0.5	0.05	0.06	0.2	0.02
	Horizontal Crown Radius - r (m)	0.5	6.5	1	1	4	0.5
	Vertical Crown Radius - b (m)	0.5	6.5	2	1	3	1
	Height to Crown Center - h (m)	4	14	2	11	15	1
	Height Distribution - dh (m)	5	25	5	6	20	2
	Slope - α (°)	0	60	10	0	20	5
	Aspect - φ (°)	0	315	45	0	315	45
	Size of parameter set		829440			302400	

Structural parameters were retrieved in the second MFM stage (Fig. 1). The MFM look-up table algorithm searches the look-up table for modeled reflectance values that were within a predefined spectral range from the image reflectance from all SPOT image bands for each pixel. The spectral range was defined using the relative root mean square error (RMSE) between measured (ρ_i) and modeled (ρ_m) reflectance for the number of image bands (n_b) (Weiss et al., 2000):

$$RMSE = \sqrt{\frac{1}{n_b}\sum_{i=1}^{nb}\left(\frac{\rho_i - \rho_m}{\rho_i}\right)^2} \quad (1)$$

The structural parameters associated with the matching modeled reflectance values within the spectral range were then selected as potential inversion results and further refined by ensuring that the slope and aspect of a given pixel matched the slope and aspect parameters used to generate the look-up table record. The distribution of potential inversion results contained the following structural parameters of interest: stem density (λ), horizontal crown radius (*r*), vertical crown radius (*b*) and species.

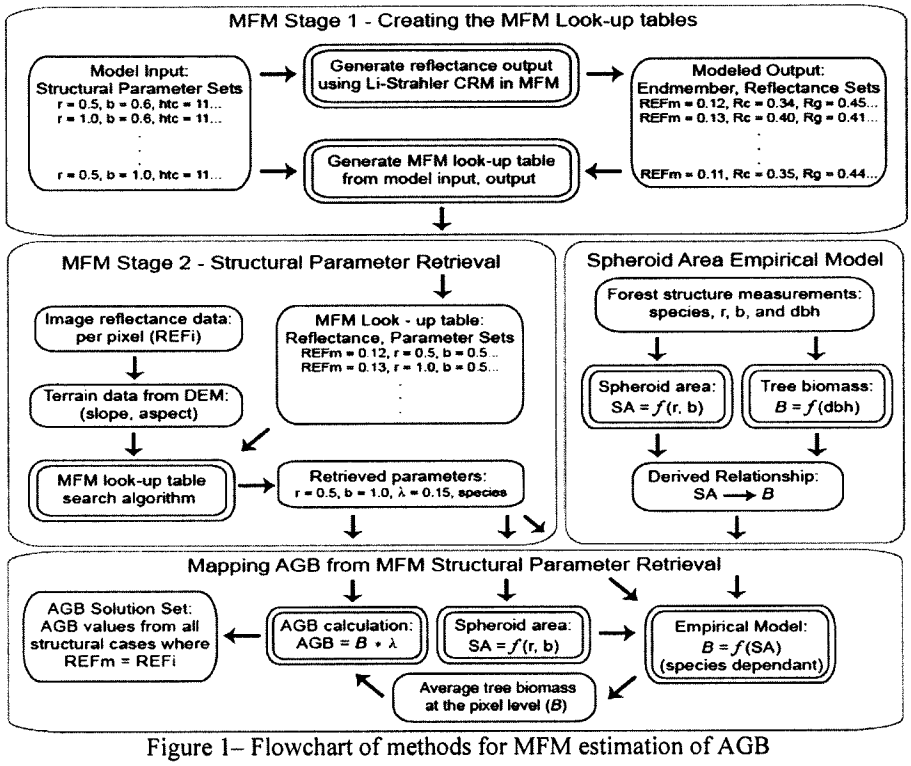

Figure 1– Flowchart of methods for MFM estimation of AGB

Estimating tree biomass from a crown spheroid area based empirical model

A regression model was created to relate *r* and *b* parameters, summarized as crown surface area (SA), to tree biomass for stands of uniform age (Fig. 1). The *r* and *b* parameters were selected for the biomass model instead of height to crown because they can be more accurately predicted due to their influence on the relative proportions of the primary drivers of pixel level reflectance: sunlit and shadowed canopy and ground area. Crown SA was related to biomass as an analogue to the area of the crown supporting physiological processes. Surface area was calculated using maximum horizontal and vertical crown radial extent within spheroid area equations. A new SA-based tree biomass allometric equation was created for both conifer and deciduous trees using linear least squares regression. Regression models were generated using a dataset consisting of field measurements of crown dimensions (*r*, *b*) and previous calculations of tree biomass from the dbh-based log-transformed power model for 350 individual trees from each species type.

AGB estimation from MFM structural parameter retrieval

After calculating SA from the estimates of *r* and *b* in each set within the distribution of retrieved structural parameters from the second stage MFM estimates of crown dimension, the SA-based allometric equations were applied to predict average tree biomass within the area covered by the image pixel (Fig. 1). Average tree biomass was then aggregated to total biomass for all trees within the area covered by the pixel by multiplying the estimate of λ, in units of trees per unit area, by the average tree biomass ($AGB = B \cdot \lambda$). The result was a set of solutions of potential AGB for the pixel area. The values written to the output image and used for validation were summarized from the solution set using the median value, which has been shown to be the most suitable statistic for solution distributions (Weiss et al., 2000).

AGB estimation from NDVI and SMA fractions

For comparative purposes, biomass density was estimated using empirical relationships with the NDVI (Rouse et al., 1974) and spectral mixture analysis (SMA, Adams et al. 1993) sub-pixel scale shadow endmember fractions. These have been used extensively and reported as effective predictors in past studies (Zheng et al., 2004; Peddle et al., 1999). The NDVI was calculated using SPOT red (band 2) and NIR

(band 3) reflectance values (equation: [band 3- band 2] / [band 3+ band 2]). The SMA used the ENVI linear unmixing module (RSI, 2006) with endmember spectra collected in the field to determine the relative abundance of sub-pixel shadow for the SPOT imagery (the same endmember values were used for both SMA and MFM). Shadow (S) fraction was used based on previous research that has showed S as both theoretically and empirically superior to canopy and background fractions (Hall et al., 1995, Peddle et al., 1999, 2001a). AGB as a function (separately) of NDVI and SMA was modeled using leave-one-out cross-validation methods. The cross-validation involved iteratively removing one AGB validation plot, fitting the regression equation to the remainder of the plots and applying the equation to predict AGB for the "left-out" plot. This was repeated for each plot in the sample, from which the predictive equations were aggregated.

RESULTS

Field Measured forest stand structure and biomass

Stand age within the study area was typically between 90 to 120 years for conifer stands and 50 to 90 years for deciduous stands. Trembling aspen trees in the study area were, on average, slightly larger than the lodegpole pine, with an average dbh of 18.8 cm and 17.3cm, respectively. The height distributions, however, were similar between the two species with mean conifer stand height only 0.5m greater than deciduous stand height (Table 2). Minimum and maximum measured stem density was 725 stems/ha and 3025 stems/ha respectively. The majority of validation plots within the study area had measured density which ranged from 800 to 1600 stems/ha with higher densities on average occurring within conifer dominant stands (Table 2). Vertical crown radius ranged from 0.4 to 8.4m and was typically larger and more variable in conifer stands than in deciduous stands. The range of horizontal crown radius was similar between the two species types, although deciduous stands had a larger *r* on average. The average conifer stand AGB (141 t/ha) was lower than deciduous stand AGB (155 t/ha). The range of AGB was also wider for deciduous stands than for the conifer stands (Table 2).

Table 2 - Descriptive statistics for field measured horizontal crown radius (r), vertical crown radius (b), tree height (h), diameter at breast height (dbh), stem density (λ), and AGB measured within lodgepole pine and trembling aspen validation plots.

		r (m)	b (m)	h (m)	dbh (cm)	λ (stems/ha)	Biomass (t/ha)
Lodgepole	**Mean**	1.0	3.0	15.1	17.3	1500	141
Pine	**S.D.**	0.4	1.2	3.3	5.4	600	34
Plots = 21	**Minimum**	0.2	0.5	4.3	5.0	775	73
Trees = 1221	**Maximum**	3.1	8.4	24.7	34.8	3025	213
Trembling	**Mean**	1.6	1.6	14.6	18.8	1200	155
Aspen	**S.D.**	0.6	0.8	3.2	5.1	400	46
Plots = 15	**Minimum**	0.3	0.4	7.9	8.1	725	67
Trees = 667	**Maximum**	3.4	4.3	22.9	37.2	1850	243

AGB and biomass density models

Using the tree biomass data and crown surface area calculated from *r* and *b*, new tree-biomass allometric equations were fit based on the observed linear relationship for both lodgepole pine (Fig. 2a) and trembling aspen (Fig. 2b) species. The crown SA data were related to tree biomass with an $r^2 = 0.63$ and RMSE = 32.7 t/ha for lodgepole pine trees and an $r^2 = 0.52$ and RMSE = 69.8 t/ha for trembling aspen trees (Table 3). The RMSE values observed in these new crown SA models were higher than the RMSE reported for the same species based on dbh models (Case and Hall, *in* review) or height and dbh models (Singh, 1982), however, the crown SA models were most appropriate for use with the output from the MFM-GOMS inversion due to the accurate *b* and *r* predictions (Soenen et al., 2007b).

Table 3 - Regression parameters, predictive strength (r^2) and standard error (S.E.) for crown surface area vs. calculated individual tree biomass for lodgepole pine and trembling aspen. p-value < 0.05.

	n	b_0	b_1	r^2	S.E.
Lodgepole pine	350	21.000	2.337	0.63	32.7 t/ha
Trembling Aspen	350	17.121	4.388	0.52	69.8 t/ha

Forest stand structure estimates from MFM inversion

Estimates of density obtained through MFM inversion were most accurate when a look-up table constrained by field observations (Table 1) and a smaller discrete increment through the structural parameter range was used (i.e. constrained LUT). Using these finer constrained look-up tables, average prediction error determined by absolute RMSE for density estimates was 590 stems/ha for lodegepole pine validation plots and 310 stems/ha for trembling aspen dominant validation plots. The relative absolute error was 40% for lodgepole pine and 27% for trembling aspen. In comparison, Wu and Strahler (1994) predicted stem density for nine lower-density conifer dominant stands over less variable terrain at 18% relative absolute error. The average prediction error for density estimates obtained from the unconstrained LUT, created using general structural inputs, was 1050 stems/ha for lodgepole pine validation plots and 530 stems/ha for trembling aspen. The trembling aspen estimate error was similar in magnitude to the precision, or discrete increment size of density within the look-up tables used for retrieval. This was expected since it was unlikely that the minimum average error would surpass the precision or increment size of the LUTs used in the estimation technique. Lodgepole pine estimate error, however, was approximately double the increment size indicating that the precision of the LUT was not the limiting factor on the minimum average error.

Average prediction error for conifer r and b was 0.4m and 0.8m RMSE, respectively, using the constrained LUT. Using the unconstrained LUT, prediction error increased to 1.1m for r and 1.2m for b. Prediction error for deciduous r and b was 0.4 and 0.9m RMSE, respectively, using the constrained LUTs and 0.9m and 1.0m RMSE using the unconstrained LUTs. Thus, LUTs using *a priori* knowledge of field conditions and smaller increment sizes were most effective at accurately predicting crown structure and reducing input error in subsequent biomass modeling.

Mapping forest AGB using MFM inversion

Results from using structural estimates from the MFM inversion within the biomass prediction model (Table 4) showed the lowest overall error (RMSE = 33.2 t/ha) for lodgepole pine plots was similar to SMA (RMSE = 32.9 t/ha) and lower than NDVI (RMSE = 34.6 t/ha). The absolute average prediction error was also similar between the prediction methods, with the MFM inversion method producing the most accurate estimates. The error results for trembling aspen validation plots were similar to the lodgepole pine plots, with the MFM inversion method resulting in RMSE and absolute error values similar to the empirical methods (Table 4).

Table 4 – Root mean square error (RMSE) and absolute average prediction error (x) for biomass estimates within the validation plots.

	MFM Inversion		NDVI		Shadow Fraction	
	RMSE	**x**	**RMSE**	**x**	**RMSE**	**x**
Lodgepole Pine	33.2 t/ha	24.6 t/ha	34.6 t/ha	28.1 t/ha	32.9 t/ha	25.1 t/ha
Trembling Aspen	52.5 t/ha	43.6 t/ha	53.1 t/ha	41.3 t/ha	50.0 t/ha	40.5 t/ha

The prediction error for these methods was within 40 t/ha for conifer validation plots. Although direct comparisons with other studies elsewhere cannot be made definitively, we note that this level of error is similar to validation RMSE of 37.6 t/ha reported by Hall et al. (2006) for a Boreal study area, less accurate than the 20t/ha difference reported by Hall et al. (1995) in another Boreal application and the 18 t/ha in an mixed forest application reported by Peddle et al. (2003). In our study, the absolute RMSE for all methods was higher than the error at the majority of the validation plots. This would indicate that there

were a small number of plots with large differences between estimated and measured biomass density that increased the overall average.

Error levels for a minority of plots were considerably higher than average in both conifer and deciduous validaton sets. In particular, the prediction errors for three of the lodgepole pine validation plots were consistently high (> 60 t/ha) regardless of prediction method. The majority of the remaining lodgepole pine validation plots had error values less than 40 t/ha. The maximum difference between estimated and measured biomass using the MFM inversion method was 164 t/ha while the minimum was 0 t/ha. The overall error was affected by a few plots with error levels considerably larger than the majority. Of the 21 validation plots, 13 fell within a difference of 20t/ha, and 18 fell within a difference of 40t/ha. There were also plots within the deciduous validation set where the difference between measured and estimated values was considerably larger than the average. The maximum difference was 96t/ha and minimum difference was 4t/ha. There were 3 validation plots of the 15 within 20t/ha while 8 were within 40t/ha. There was no observed trend in error (e.g. overestimation, underestimation) in either the conifer or deciduous results.

It is interesting to note that the magnitude of error for many of the validation plots was similar regardless of biomass estimation method. There were, however, a few exceptions. In two other validation plots, for example, the error for the MFM spectral domain method was significantly lower than the NDVI and SMA methods. These validation plots both had relatively low measured biomass densities, suggesting that the NDVI and SMA methods were unsuitable for forest stands with lower biomass densities (Fig. 2, 3). The canopy reflectance model based methods appeared to perform well across a greater range of forest stand types and conditions.

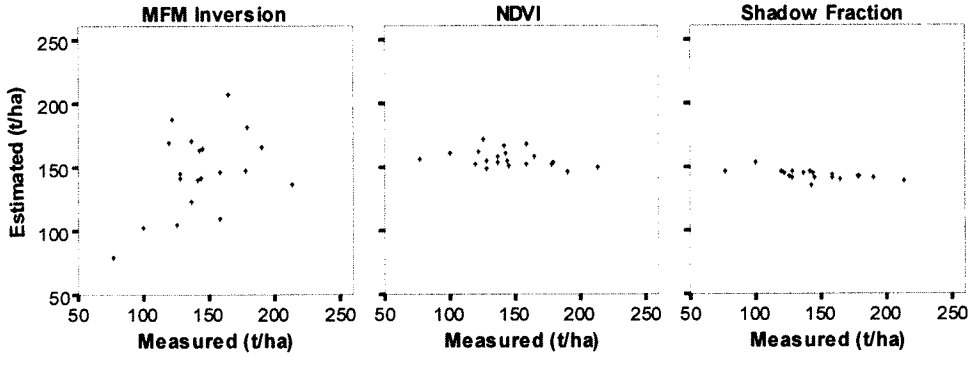

Figure 2 - Conifer biomass estimated through MFM inversion (a), NDVI (b), and mixture analysis shadow fraction (c), plotted against biomass calculated from field data.

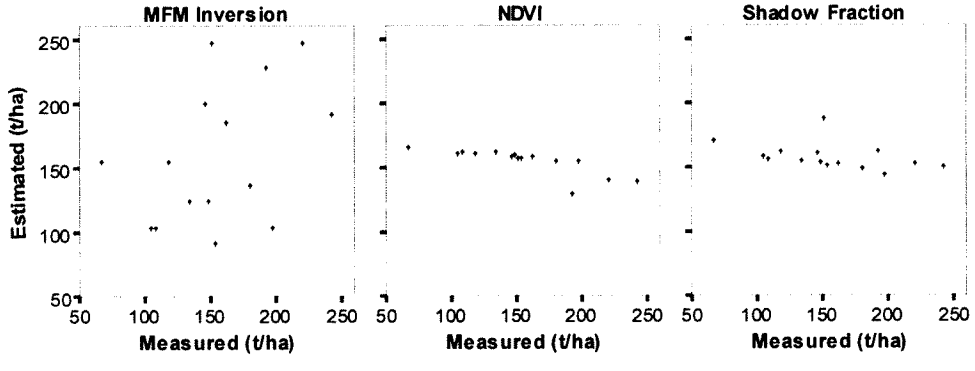

Figure 3 - Deciduous biomass estimated through MFM inversion (a), NDVI (b), and mixture analysis shadow fraction (c), plotted against biomass calculated from field data.

Mapping of AGB with MFM Inversion

The spatial patterns of biomass density (Fig. 4) were, as expected, with low values found near roads, trails, cut-lines and cut-blocks, and higher biomass density values found primarily on north-northwest facing slopes and in high density lodgepole pine stands. The biomass mapping algorithm was effective in masking areas with little or no biomass including rivers, roads, rocky slopes and Barrier lake, however, the algorithm also masked areas of deep topographic shadowing. This erroneous masking, while not significant in extent, would have some effect on any subsequent biomass accounting.

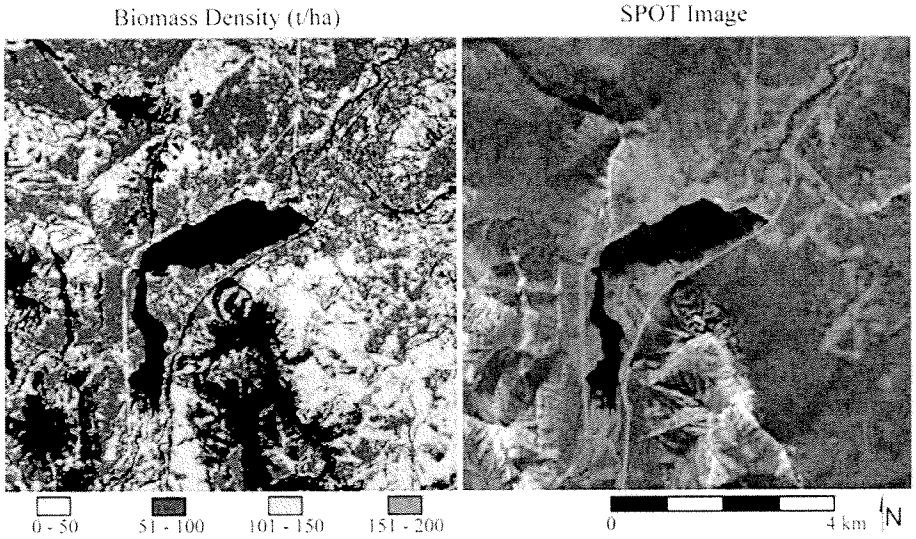

Figure 4 – SPOT image (right: bands 3,2,1) and map of forest biomass density from MFM inversion, with results aggregated to 50 t/ha classes, black represents areas with no inversion results.

DISCUSSION

Advancements and advantages of the MFM inversion method

The MFM inversion method for biomass density has advanced the MFM biophysical parameter estimation methodology by extending the capabilities toward prediction of second-order forest stand attributes that are not able to be directly derived from satellite imagery. The results show that the MFM method was suitable for making estimates of forest stand biomass density from multispectral image data, and the level of accuracy was equivalent to, or surpassed other procedures that employ empirical methods (SMA, NDVI). Furthermore, the MFM inversion method has several key advantages such as use of more refined parameter classes with flexible class ranges and increments, the explicit physical parameterisation of sun-surface-sensor geometry as well as forest stand attributes, the suitability to multi-image studies (different seasons and solar/view geometries are handled explicitly), and, perhaps most importantly, the ability to function fully with minimal or no field or *a priori* information (Peddle et al., 2007).

With the canopy reflectance model inversion procedure, it is possible to operate with little or no field data providing that the physical relationship between first-order canopy variables and the parameter of interest (e.g. biomass) is defined. Conversely, to construct an empirical model, the linear regression methods require that a spatially representative sample of the structural parameter of interest be acquired from the field. For large-areas, particularly those that include remote, inaccessible terrain (Turner et al., 2004), the required resources are likely excessive and impractical, yet the increased variation for a given parameter makes a larger sample size essential for valid statistical testing.

The minimum requirement for operation of the canopy reflectance model inversion method is spectral information for the primary overstory species, understory background, and shadowed vegetation. These spectral signatures can be measured in the field, extracted directly from the imagery, obtained from

spectral libraries, or modeled, with hybrid approaches also feasible (e.g. Peddle et al., 1999). If, however, spectral signatures for endmembers are not available, MFM can determine these inputs internally based on progressively increasing the precision of spectral ranges, similar to any other parameter. It should also be noted that, when *a priori* structural or other information is available, there are no constraints imposed, and even general structural information can increase estimation accuracy by constraining input ranges within the canopy reflectance model inversion method. This also results in faster computing times.

The minimal field data requirements of the MFM inversion procedure also have forest management implications since it is possible to characterize and map large swaths of forested area with limited field measurements. The MFM method is scalable to coarser resolution data which allows larger areas of interest to be considered and may provide information about spatial distribution of AGB and how it relates to topography and forest stand characteristics.

Within the study, unknown error introduced through error in tree measurements and inherent error within the dbh-based biomass model is likely to have propagated through to the MFM inversion estimates. While determining the source and extent of this error is beyond the scope of this study, it is important to acknowledge the existence of these potential errors that are external to the MFM modeling domain.

CONCLUSIONS

A new method was presented for estimating forest biomass which extends the capabilities of the existing MFM canopy reflectance model inversion toward deriving second-order parameters that cannot be directly estimated from satellite imagery. The method uses indirect look-up table based canopy reflectance model inversion to obtain estimates of canopy dimensions and stand density. These first-order parameters are then related to biomass through empirical modeling. This method has significant advantages over traditional empirical estimation methods since it does not require extensive field sampling and provides additional important structural information. Conceptually, the approach developed here provides flexibility and power within a canopy reflectance model inversion context for deriving detailed biophysical information.

In terms of the study hypothesis that MFM inversion would generate more accurate predictions of forest biomass, this was partially achieved in terms of validation against independent field data. The MFM biomass density estimation error provided a marginal improvement or was similar to the empirical NDVI and SMA methods, but offered considerable unique advantages in terms of flexibility, reduced field requirements, suitability for larger areas involving multi-image/multi-temporal/multi-sensor data, and unparalleled robustness of processing and analysis.

ACKNOWLEDGEMENTS

This research was supported in part by grants to Dr. Peddle and collaboration from the Natural Sciences and Engineering Research Council of Canada (NSERC), Alberta Ingenuity Centre for Water Research (AICWR), Prairie Adaptation Research Collaborative (PARC), Water Institute for Semiarid Ecosystems (WISE), Natural Resources Canada, NASA Goddard Space Flight Centre/University of Maryland, Alberta Research Excellence Program, Miistakis Institute of the Rockies (DEM), Center for Remote Sensing, Boston University (GOMS model) and the University of Lethbridge. Computing resources were provided through the Western Canada Research Grid (WestGrid NETERA c3.ca). SPOT imagery was acquired from Iunctus Geomatics Corporation and the Alberta Terrestrial Imaging Centre (ATIC), both of Lethbridge Alberta. We are grateful to Sam Lieff, Adam Minke and Kristin Yaehne for field assistance and the staff at the Kananaskis Field Stations for logistical support in the field.

REFERENCES

Adams, J. B., Smith, M. O.,&Gillespie, A. R. (1993). Imaging spectroscopy: Interpretation based on spectral mixture analysis. In C. M. Pieters & P. Englert (Eds.), *Remote geochemical analysis: Elemental and mineralogical composition* (pp. 145-166). New York: Cambridge University Press.

Alberta Environmental Protection (1991). Alberta Vegetation Inventory Standards Manual V. 2.1. Alberta Environmental Protection, Resource Data Division, Data Acquisition Branch, Edmonton, Alta..

Archibald, J.H., G.D. Klappstein, and I.G.W. Corns (1996). *Field guide to ecosites of southwestern Alberta*. UBC Press, Vancouver.

ASD (1998). Fieldspec FR User's Guide. Analytical Spectral Devices Inc., Boulder, pp. 1-47.

Baskerville, G.L. (1972). Use of Logarithmic Regression in Estimation of Plant Biomass. *Canadian Journal of Forestry*. 2: 49 – 53.

Brown, S. (2002). Measuring Carbon in Forests: Current Status and Future Challenges. *Environmental Pollution*, 116: 363 – 372.

Case, B.S., and R.J. Hall (2007) Assessing prediction errors of generalized tree biomass and volume equations for the boreal forest region of West-Central Canada. (in review).

Chen, J.M., X. Li, T. Nilson, A. Strahler (2000). Recent Advances in Geometrical Optical Modelling and its Applications. *Remote Sensing Reviews*, 18: 227 – 262.

Cihlar, J., S. Denning, F. Ahern, O. Anno, A. Belward, F. Bretherton, W.Cramer, G. Dedieu, C. Field, R. Francey, R. Gommes, J. Gosz, K. Hibbard, T. Igarashi, P. Kabat, D. Olsen, S. Plummer, I. Rasool, M. Raupach, R. Scholes, J. Townshend, R. Valentini, and D. Wickland (2002). Initiative to Quantify Terrestrial Carbon Sources and Sinks. *EOS Transactions*, 83(1): 6-7.

Elvidge, C.D., R.J.P. Lyon (1985). Influence of Rock-Soil Spectral Variation on the Assesment of Green Biomass. *Remote Sensing of Environment*, 17: 265 – 279.

Foody, G.M., D.S. Boyd, and M.E.J. Cutler (2000). Predictive relations of tropical forest biomass from Landsat TM data and their transferability between regions. *Remote Sensing of Environment*, 85: 463 – 474.

Franklin, S.E., R.J. Hall, L.Smith, G.R. Gerylo (2003). Discrimination of Conifer Height, Age, and Crown Closure Classes using Landsat-5 TM Imagery in the Canadian Northwest Territories. *International Journal of Remote Sensing*, 24(9): 1823 – 1834.

Gemmell, F. (1995). Effects of Forest Cover, Terrain, and Scale on Timber Volume Estimation with Thematic Mapper Data in a Rocky Mountain Site. *Remote Sensing of Environment*, 51: 291 – 305.

Gemmell, F. (1998). An Investigation of Terrain Effects on the Inversion of a Forest Reflectance Model. *Remote Sensing of Environment*, 65: 155 – 168.

Gerylo, G.R., R.J. Hall, S.E. Franklin, and L. Smith (2002). Empirical Relations Between Landsat TM Spectral Response and Forest Stands near Fort Simpson, Northwest Territories, Canada. *Canadian Journal of Remote Sensing*, 28: 68 – 79.

Hall, F.G., Y.E. Shimabukuro, K.F. Huemmerich (1995). Remote Sensing of Forest Biophysical Structure using Mixture Decomposition and Geometric Reflectance Models. *Ecological Applications*. 5(4): p. 993 – 1013.

Hall, R.J., R.S. Skakun, E.J. Arsenault, and B.S. Case (2006). Modeling Forest Stand Structure Attributes Using Landsat ETM+ data: Application to Mapping of Aboveground Biomass and Stand Volume. *Forest Ecology and Management*, 225: 378 – 390.

Hame, T., A. Salli, K. Andersson, A. Lohi (1997). A New Methodology for the Estimation of Biomass of Conifer-Dominated Boreal Forest Using NOAA AVHRR data. *International Journal of Remote Sensing*, 18(15): 3211 – 3243.

Hyyppä, J., H. Hyyppä, M. Inkinen, M. Engdahl, S. Linko, Y-H. Zhu (2000). Accuracy comparison of various remote sensing data sources in the retrieval of forest stand attributes. *Forest Ecology and Management*, 128: 109 – 120.

Kimes, D.S., Y. Knyazikhin, J. Privette, A. Abuelgasim, and F. Gao (2000). Inversion Methods for Physically Based Models. *Remote Sensing Reviews*, 18: 381 – 440.

Kurz, W.A., M.J. Apps (1999). A 70-year Retrospective Analysis of Carbon Fluxes in the Canadian Forest Sector. *Ecological Applications*, 9: 526 – 547.

Li, Xiaowen and A.H. Strahler (1992). Geometric-Optical Bidirectional Reflectance Modeling of the Discrete Crown Vegetation Canopy: Effect of Crown Shape and Mutual Shadowing. *IEEE Transactions on Geoscience and Remote Sensing*, 30: 276 – 292.

Lu, D. (2006). The potential and challenge of remote sensing-based biomass estimation. Review article. *International Journal of Remote Sensing*, 27: 1297 – 1328.

Milton, E. J., K. Lawless, A. Roberts, and S. E. Franklin, (1997). The effect of unresolved scene elements on the spectral response of calibration targets: an example, Canadian Journal of Remote Sensing, 23(3): 126-130.

Patenaude, G., R. Milne, T.P. Dawson (2005). Synthesis of Remote Sensing Approaches for Forest Carbon Estimation: Reporting to the Kyoto Protocol. *Environmental Science and Policy*, 8: 161 – 178.

Palacios-Orueta, A., E. Chuvieco, A. Parra, and C. Carmona-Moreno (2005). Biomass Burning Emissions: A Review of Models Using Remote Sensing Data. *Environmental Monitoring and Assessment*. 104: 189 – 209.

Peddle, D.R., F.G. Hall, E.F. LeDrew (1999). Spectral Mixture Analysis and Geometric-Optical Reflectance Modelling of Boreal Forest Biophysical Structure. *Remote Sensing of Environement*, 67: 288 – 297.

Peddle, D.R., S.P. Brunke and F.G. Hall (2001a). A Comparison of Spectral Mixture Analysis and Ten Vegetation Indices for Estimating Boreal Forest Biophysical Information from Airborne Data. *Canadian Journal of Remote Sensing*, 27(6): 627 – 635.

Peddle, D.R., H.P. White, R.J. Soffer, J.R. Miller, E.F. LeDrew (2001b). Reflectance Processing of Remote Sensing Spectroradiometer Data. *Computers and Geosciences*, 27: 203 – 213.

Peddle, D.R., S.E. Franklin, R.L. Johnson, M.A. Lavigne, and M.A. Wulder (2003). Structural Change Detection in a Disturbed Conifer Forest Using a Geometric Optical Reflectance Model in Multiple Forward Mode. *IEEE Transactions in Geoscience and Remote Sensing*, 41(1): 163 – 166.

Peddle, D.R., R.L. Johnson, J.Cihlar, and R. Latifovic (2004). Large Area Forest Classification and Biophysical Parameter Estimation Using the 5-Scale Canopy Reflectance Model in Multiple Forward Mode. *Remote Sensing of Environment. BOREAS Special Issue*, 89: 252 - 263.

Peddle, D.R., R.L. Johnson, J.Cihlar, S.G. Leblanc, J.M. Chen and F.G. Hall (2007). MFM-5-Scale: A Physically Based Inversion Modelling Approach for Unsupervised Cluster Labelling and Independent Forest Landcover Classification. *Canadian Journal of Remote Sensing*, 33(3): 214-225.

Rosenqvist, A., A. Milne, R. Lucas, M. Imhoff, C. Dobson (2003). A Review of Remote Sensing Technology in Support of the Kyoto Protocol. *Environmental Science & Policy*, 6: 441 – 455.

Rouse, J. W., R.H. Haas, D.W. Deering, and J.A. Sehell (1974). Monitoring the vernal advancement and retrogradation (Green wave effect) of natural vegetation. Final Rep. RSC 1978-4, Remote Sensing Center, Texas A&M Univ., College Station.

Singh, T. (1982). Biomass Equations for Ten Major Tree Species of the Prairie Provinces. Canadian Forest Service, Northern Forest Research Centre, Edmonton, Alta. Information Report NOR-X-242.

Smith, G.M., E.J. Milton (1999). The Use of the Empirical Line Method to Calibrate Remotely Sensed Data to Reflectance. *International Journal of Remote Sensing*, 20: 2653 – 2662.

Soenen, S.A., D.R. Peddle, and C.A. Coburn (2005). SCS+C: A Modified Sun-Canopy-Sensor Topographic Correction in Forested Terrain. *IEEE Transactions on Geoscience and Remote Sensing*, 43: 2148 - 2159.

Soenen, S.A., D.R. Peddle, C.A. Coburn, R.J. Hall and F.G. Hall (2007a). Improved Topographic Correction of Forest Image Data using a 3-D Canopy Reflectance Model in Multiple Forward Mode. *International Journal of Remote Sensing*, (in press).

Soenen, S.A. D.R. Peddle, C.A. Coburn, R.J. Hall and F.G. Hall (2007b). Canopy Reflectance Model Inversion in Multiple Forward Mode: Analysis of Multiple Solution Sets. *Photogrammetric Engineering and Remote Sensing*, (in press)

Woodcock, C.E., J.B. Collins, V.D. Jakabhazy, X. Li, S.A. Macomber, and Y. Wu (1997). Inversion of the Li-Strahler Canopy Reflectance Model for Mapping Forest Structure. *IEEE Transactions on Geoscience and Remote Sensing*, 2: 405 – 414.

Wu, Y., A. H. Strahler (1994). Remote Estimation of Crown Size, Stand Density, and Biomass on the Oregon Transect. *Ecological Applications*, (4)2: 299 – 312.

Wulder, M.A. (1998). Optical Remote Sensing Techniques for the Assesment of Forest Inventory and Biophysical Paramters. *Progress in Physical Geography*, 22: 449 -476.

Zheng, D., J. Rademacher, J. Chen, T. Crow, M. Bresee, J. Le Moine, S. Ryu (2004). Estimating Aboveground Biomass using Landsat 7 ETM+ Data Across a Managed Landscape in Northern Wisconsin, USA. *Remote Sensing of Environment*. 93: 402 – 411.

CRSS/ASPRS 2007 Specialty Conference

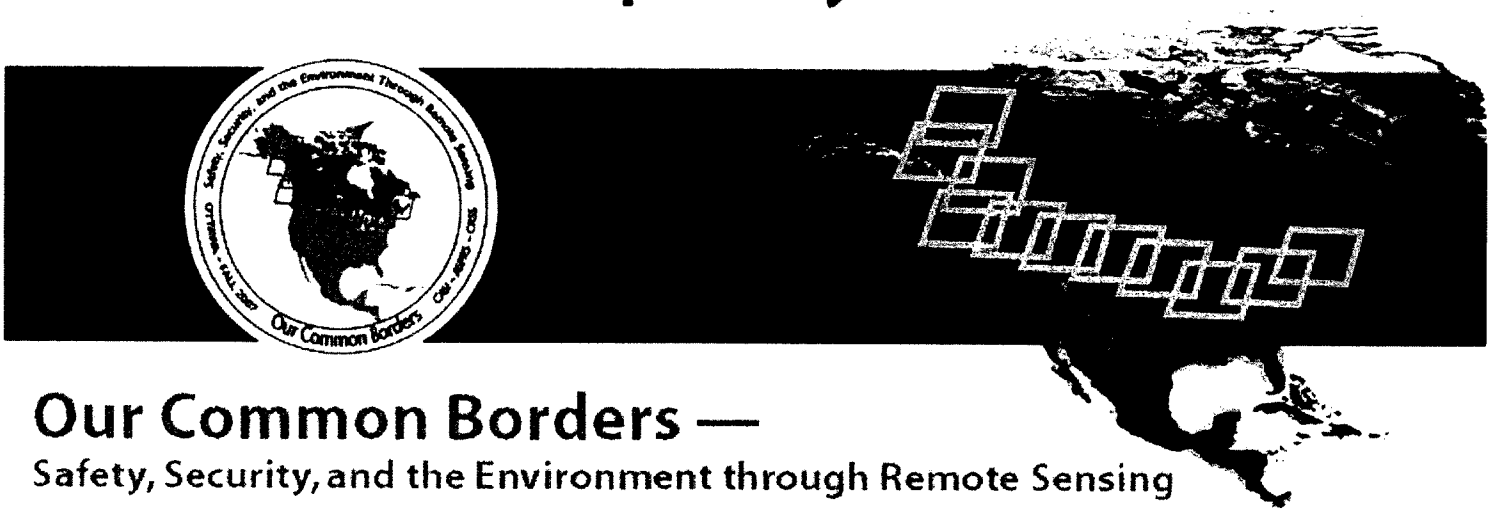

Our Common Borders —
Safety, Security, and the Environment through Remote Sensing

Westin Hotel Ottawa
October 28 - November 1, 2007
Ottawa, Canada

Proceedings Papers Download
Table of Contents
Author Index
Copyright

Co-sponsors:

asprs
THE IMAGING & GEOSPATIAL INFORMATION SOCIETY

Ottawa 2007 Proceedings (Members Only)

Non-member attendees please go here

As a convenience to ASPRS members, the Ottawa 2007 annual conference proceedings have been made available

To see the table of contents and to view/download/print proceedings articles:

- If you are already logged in simply click the link below
- If you are not already logged in please do so by entering your ASPRS member ID and password in the text boxes in the top right corner of this page. Then click the link below.

LOG IN FIRST Then go to Ottawa 2007 Proceedings Table of Contents

5410 Grosvenor Lane, Suite 210, Bethesda, Maryland 20814-2160